

Modeling and analysis of the impact of degree of membrane rejection on polarization modulus

Sergey P. Agashichev

National Energy and Water Research Center, ADWEA, PO Box 54111, Abu Dhabi, UAE
Fax +971 (2) 665.83.74; email: spagashichev@adwea.gov.ae, agashichev@yahoo.com

Received 16 May 2010; Accepted in revised form 26 December 2010

ABSTRACT

Model describing the impact of degree of membrane rejection on behavior of concentration profile has been proposed. The model is based on the following physical assumptions: (1) the fluid was assumed to be incompressible, continuous and isothermal with uniform density field under the steady-state (time-independent) conditions; (2) transverse velocity was approximated by parabolic profile. Proposed model can be used for analysis of behavior of concentration profile. It can be applied for analysis of performance characteristics of membrane processes and laboratory- scale data at variable values of the observed degree of rejection. Sets of calculated profiles at different membrane rejection and temperature are attached.

Keywords: Concentration polarization; Degree of rejection; Modeling

1. Introduction and formulation of the problem

Pressure-driven processes are accompanied by concentration polarization (CP) that can be quantified by the degree of concentration polarization or polarization modulus that in turn, depends on hydrodynamics, physical properties and membrane characteristics. Quantitative modeling of concentration polarization is essential for design and analysis of membrane process. Many traditional models are based on combination of convection-diffusion and Navier–Stokes equations. The classical solutions for hydrodynamic and concentration profiles were proposed by Berman, Brian and Sherwood [1–3]. The studies submitted by Kleinstreuer and Karode [4–6] are examples of further implications of similar approach. Kim and Hoek, [7] proposed comparative analysis of CP based on film theory and convection- diffusion model. Wiley and Fletcher, [8], presented technique for modeling fluid dynamics. Gupta et al [9] gave relation between transport parameters, boundary layer thickness

and experimentally measurable quantities such as feed and permeate concentration using combined model for membrane transport and concentration polarization.

Recent trends in modeling can be characterized by diversification of physical assumptions underlying the model along with development and improvement of mathematical techniques. Many physical factors, such as enhancement of surface concentrations due to gel accumulation, non-Newtonian behavior of fluid and shear induced diffusion, etc. are taken into consideration by modeling. Development of new generation of computers made possible execution of more sophisticated mathematical procedures and techniques, in particular, 2-D streamline upwind finite element model for concentration polarization was considered in [10]. Non Newtonian behavior and shear-dependence of characteristics are considered in [11,12]. Enhancement of CP due to gel accumulated at the membrane was described in [13–15].

Many methods imply intrinsic membrane rejection as an input into models. Factors affecting membrane re-

jection are reviewed by Bellona and Drewes [16]. Based on analysis of published data the quantitative relation between membrane rejection and concentration profile is one of the most unresolved theoretical aspects of membrane technology, In this regard the objective of this study focuses on modeling of concentration profile depending upon degree of membrane rejection.

2. Premises and assumptions of the model

The fluid is assumed to be incompressible, continuous and isothermal with uniform density field under the steady-state (time independent) conditions. Transverse transport is based on the following mechanisms: convection due to pressure difference and back diffusion owing to concentration gradient. The illustration is shown in Fig. 1. Analysis of the CP is based on the following governing equation:

$$V_1 c + D \frac{dc}{dz} = V_2 C_2 \quad (1)$$

where V – transverse flux; D – diffusivity; and C – local concentration (see Fig. 1). The first term on the left hand side represents convective flux towards membrane; the second one describes the back diffusion.

The dimensionless variable η was used for further mathematical analysis. The dimensionless variable, η , ranges from $\eta = 0$ at the centerline to $\eta = 1$ at the membrane surface.

$$\eta = (H - z)/H \quad (2)$$

Transverse velocity, $V(\eta)$, was approximated by parabolic function based on the profile proposed by Berman, [1]:

$$V(\eta) = V_{1_MAX} \left[\frac{\eta}{2} (3 - \eta^2) \right] \quad (3)$$

Transverse velocity varies from $V_{(\eta=0)} = 0$, at the centerline to its maximum value $V_{(\eta=1)} = V_{1_MAX}$ at the surface. At the upper boundary of diffusion layer its equal to: $V_{(\eta=f)} = V_{1_MAX} [f(3-f^2)]/2$.

The transverse velocity is assumed to be constant throughout membrane and equal to V_2 (see Fig. 1).

$$V_{MEMBR} = V_{1_MAX} = V_2 \quad (4)$$

2.1. Concentration profile

Relying upon assumed transport mechanisms, the channel was subdivided into zones (A) and (B), respectively. Zone (A) covers the core of the channel that ranges from the centerline to upper boundary of diffusion layer. Within this zone the concentration remains constant being equal to C_1 . Zone (B) covers the diffusion layer of the channel that ranges from the upper boundary of diffusion layer to membrane surface. Within zone (B) the

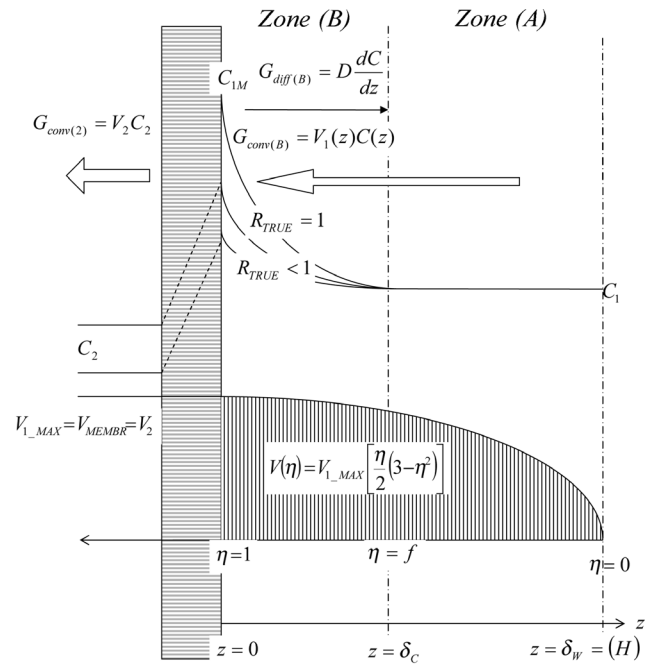


Fig. 1. Illustration of the concentration and hydrodynamic profiles.

concentration ranges from C_1 at its upper boundary to C_{1M} at the membrane surface.

The thickness of viscous layer δ_w is assumed to be equal to half-height of the channel H (Fig. 1). According to [17], the ratio of diffusion to viscous layer was assumed to be

$$\delta_c / \delta_w \approx Sc^{-1/3} \quad (5)$$

In terms of the η variable, the upper boundary of diffusion layer, f is equal to

$$f \approx 1 - Sc^{-1/3} \quad (6)$$

2.2. Membrane rejection

The degree of membrane rejection can be expressed in terms of bulk or surface concentration, they are referred to as the observed (or apparent) $R_{OBSERVED} = 1 - C_2/C_1$ and true (or intrinsic) $R_{TRUE} = 1 - C_2/C_{1M}$ degree of rejection, respectively. For the further mathematical treatment to simplify the current degree of rejection, $R(\eta)$ was introduced. It was expressed in terms of the current concentration within the boundary layer, $C(\eta)$ as follows:

$$R(\eta) = 1 - C_2 / C(\eta) \quad (7)$$

The $R(\eta)$ ranges from the observed degree of rejection expressed in terms of bulk concentration, $R_{OBSERVED}$ (C_1) to

the true degree of rejection expressed in terms of surface concentration, $R_{\text{TRUE}}(C_{1M})$.

The degree of rejection (true and observed) is related to polarization modulus α at the membrane surface as follows:

$$R_{\text{TRUE}}(\alpha_{\eta=1}) = 1 - (1 - R_{\text{OBSERVED}}) / \alpha_{\eta=1} \quad (8)$$

Relying upon analogy between mathematical formulations of the degree of rejection and concentration profiles, the $R(\eta)$ can be approximated by the exponential profile similar to $C(\eta)$.

$$R(\eta) = A \exp[B\eta] \quad (9)$$

Parameters A and B were evaluated based on the following boundary conditions

$$\begin{array}{l} \text{Membrane surface} \quad R_{(\eta=1)} = R_{\text{TRUE}} \\ \text{Upper boundary of diffusion layer} \quad R_{(\eta=f)} = R_{\text{OBSERVED}} \end{array}$$

Applying these boundary conditions it gives the parameters A and B :

$$A(\alpha, f) = R_{\text{TRUE}} / \sqrt[f-1]{R_{\text{OBSERVED}} / R_{\text{TRUE}}} \quad (10)$$

$$B(\alpha, f) = \ln(R_{\text{OBSERVED}} / R_{\text{TRUE}}) / (f - 1) \quad (11)$$

3. Modeling

The model is based on Eq. (1). The diffusion layer ranges from $z = 0$ to $z = \delta_c$ where the concentration varies from C_1 to C_{1M} and the transverse velocity from $V = V_{(\eta=f)}$ to $V = V_{\text{MAX}(\eta=1)}$. For simplification of mathematical treatment the non-dimensional variable η is used, therefore Eq. (1) can be expressed as follows:

$$V_1(\eta)C(\eta) - \frac{D}{H} \frac{dC}{d\eta} = V_2 C_2 \quad (12)$$

Boundary conditions:

$$\begin{array}{l} \text{Upper boundary of diffusion layer} \quad C_{(z=\delta_c)} = C_1 \\ \text{Membrane surface} \quad C_{(z=0)} = C_{1M} \end{array}$$

Concentration of permeate, C_2 on the right hand side of Eq. (12) can be expressed in terms of $R(\eta)$ and $C(\eta)$, see Eqs. (7) and (9).

$$C_2 = C(\eta)[1 - A \exp(B\eta)] \quad (13)$$

While the permeate flow is assumed to be equal to transmembrane flux, the right hand side of Eq. (12) can be rewritten as

$$\{V_2 C_2\} = V_{1\text{-MAX}} C(\eta)[1 - A \exp(B\eta)] \quad (14)$$

Inserting the right hand side expression, $\{V_2 C_2\}$ and transverse velocity, $\{V_{(\eta)}\}$, see Eqs. (3) and (14) respectively, into Eq. (12) we get:

$$\begin{aligned} V_{1\text{-MAX}} \left[\frac{\eta}{2} (3 - \eta^2) \right] C(\eta) - \frac{D}{H} \frac{dC}{d\eta} \\ = V_{1\text{-MAX}} C(\eta) [1 - A \exp(B\eta)] \end{aligned} \quad (15)$$

Rearrangement and separation of variables gives the following:

$$\frac{V_{1\text{-MAX}} H}{D} \left[\frac{\eta}{2} (3 - \eta^2) + A \exp(B\eta) - 1 \right] d\eta = \frac{dC}{C} \quad (16)$$

Having been integrated Eq. (16) gives

$$\begin{aligned} \frac{V_{1\text{-MAX}} H}{D} \left[0.73\eta^2 - 0.125\eta^4 - \eta + A \exp(B\eta) / B \right] \\ = \ln C + \text{const}_1 \end{aligned} \quad (17)$$

Evaluation of the constant of integration, const_1

For the const_1 to be determined, the boundary conditions at the upper surface of the diffusion layer were used, namely $C_{(\eta=f)} = C_1$, at $\eta = f = [1 - \text{Sc}^{-1/3}]$. They give the const_1 :

$$\begin{aligned} \text{const}_1 = \frac{V_{1\text{-MAX}} H}{D} \left[0.73f^2 - 0.125f^4 - f \right. \\ \left. + AB^{-1} \exp(Bf) \right] - \ln C_1 \end{aligned} \quad (18)$$

Inserting const_1 into Eq. (17) we get the following profile of concentration modulus

$$\frac{c(\eta)}{C_1} = \exp \left\{ \frac{V_{1\text{-MAX}} H}{D} \left[X(\eta) - Z(f) \right] \right\} \quad (19)$$

where

$$\begin{aligned} X(\eta) = 0.75\eta^2 - 0.125\eta^4 - \eta \\ + A(\alpha, f) [B(\alpha, f)]^{-1} \exp[B(\alpha, f)\eta] \end{aligned} \quad (20)$$

$$\begin{aligned} Z(f) = 0.75f^2 - 0.125f^4 - f \\ + A(\alpha, f) [B(\alpha, f)]^{-1} \exp[B(\alpha, f)f] \end{aligned} \quad (21)$$

for $A(f, \alpha)$, $B(f, \alpha)$ and f [see Eqs. (10), (11) and (6), respectively].

At $\eta = 1$ Eq. (19) gives the CP modulus at the membrane surface

$$\begin{aligned} \alpha_{(\eta=1)} = (C_{1M} / C_1)_{\eta=1} \\ = \exp \left\{ \frac{V_{1\text{-MAX}} H}{D} \left[X(\eta) - Z(f) \right] \right\} \end{aligned} \quad (22)$$

Being solver for $c(\eta)/C_1$, Eq. (19) gives sets of calculated profiles (see Figs. 2 and 3).

4. Implication of the model and analysis

Developed model gives analytical distribution of con-

centration at arbitrary cross section normal to membrane. It permits quantitative relationship between concentration modulus and temperature, degree of membrane rejection, specific membrane permeability and physical properties of the solution. Set of calculated profiles at different degree of membrane rejection is shown in Fig. 2. It is shown that membranes with high degree of rejection are more vulnerable to growth of surface concentration. This aspect must be taken carefully into consideration in design and analyzing experimental data on membrane with high degree of rejection and elevated feed salinity.

Impact of temperature was accounted through temperature-dependence of physical properties namely: viscosity — $\mu(t)$; diffusivity — $D(t)$, Sc-number $Sc(t)$; thickness of diffusion layer $f(t) \approx Sc(t)^{-1/3}$. Behavior of the model is shown in Figs. 2 and 3 must be taken into consideration in design and analysis of RO at elevated temperature in particular within the RO/MSF hybrid schemes where cooling water from heat rejection section is used as a feed for RO. For these schemes the preference should be given to membranes with moderate salt rejection rather than membrane with high salt rejections.

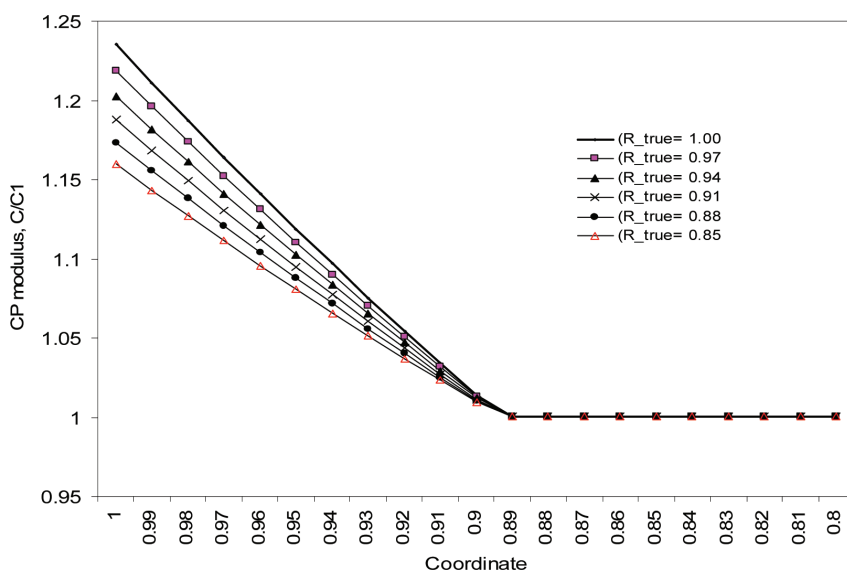


Fig. 2. Concentration profile at different degree of rejection [Set of calculated profiles based on Eq. 19]. Input data $t = 20^\circ\text{C}$; $D(t = 20) = 1.34 \times 10^{-9} \text{ m}^2/\text{s}$; $A_{\text{MEMBR}}(t = 20) = 1.3 \times 10^{-7} \text{ m}^3/[\text{m}^2\text{-s-bar}]$; $Sc(t = 20) = 814$ ($f \sim 0.89$); $H = 10^{-3} \text{ m}$.

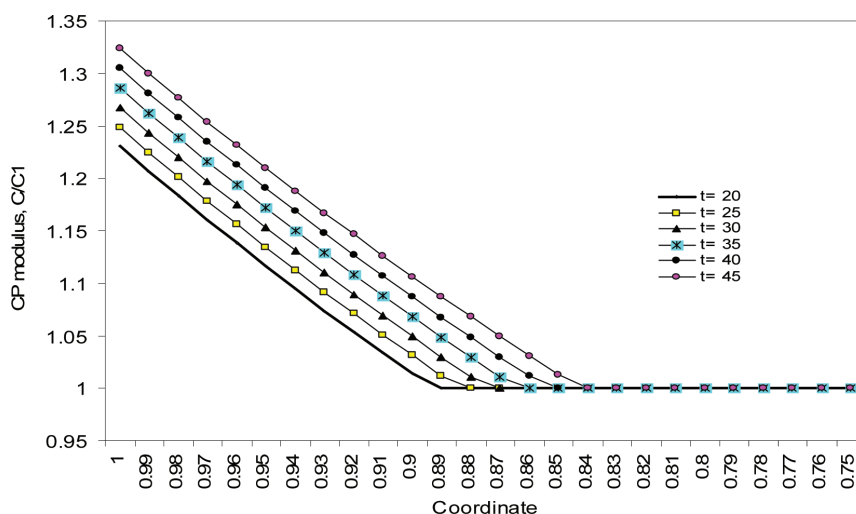


Fig. 3. Concentration profile at different temperature [Set of calculated projections based on Eq. 19]. Input data: $D(t = 20) = 1.34 \times 10^{-9} \text{ m}^2/\text{s}$; $A_{\text{MEMBR}}(t = 20) = 1.3 \times 10^{-7} \text{ m}^3/[\text{m}^2\text{-s-bar}]$; the Schmidt number ranges from $Sc(t = 20) = 814$ (where $f \sim 0.89$) to $Sc(t = 45) = 255$ (where $f \sim 0.84$); $R_{\text{EXPERIMENT}} = 0.98$; $H = 10^{-3} \text{ m}$.

5. Validation of the model and conclusions

Indirectly the correlation between the net driving force and CP degree versus operating temperature can be developed using the following experimental results: observed permeability at operating temperature – $V_M(t, \alpha)$; hydraulic membrane permeability or membrane constant – $A_M(t)$; operating pressure – ΔP and seasonal distribution of operating temperature – t . The following equations were used for interpretation of experimental results.

$$V_M(t, \alpha) = A_M(t) [\Delta P - \pi_M(t)] \tag{23}$$

$$\pi_M(t) = i\alpha(t)C_1R(273 + t) \tag{24}$$

where π_M – osmotic pressure at membrane surface, $\pi_M(t) = \alpha(t) \pi_{BULK}(t)$.

Experimental values of observed permeability, $V_M(t, \alpha)$, were normalized to the reference temperature being multiplied by the viscosity-correction factor – $\mu_t/\mu_{(t=25)}$. Combining Eqs. (23) and (24) and using experimental data on temperature, operating pressure, observed permeability, we get the quantitative relation between CP modulus $\alpha(t)$ and operating temperature – t . Experimentally-based profiles of the net driving force $[\Delta P - \pi_M(t)]$ and CP modulus $\alpha(t)$ are shown in Fig. 4.

$$\alpha(t) = \left[\frac{\Delta P - V_M(t, \alpha)\mu(t)}{A_{M(t)}\mu_{(t)}} \right] / [iC_1R(273 + t)] \tag{25}$$

Behavior of the theoretical and experimentally-based polarization modulus $\alpha(t)$ against temperature is shown in Fig. 5. Variability and accuracy of the experimentally-based module were characterized by means of true standard deviation $\sigma(\alpha)$ as follows:

$$\sigma(\alpha) = \sqrt{\frac{\sum(\alpha_i - \bar{\alpha})^2}{n}} \tag{26}$$

The standard deviation was estimated to be $\sigma(\alpha) = 0.02554$. Average difference between experimental and model values does not exceed 12%.

Based on analysis of experimental data and calculated results the following conclusions have been drawn:

1. Growth of degree of membrane rejection is accompanied by increase of surface concentration and CP modulus;
2. Growth of temperature is accompanied by growth of surface concentration and CP modulus at membrane surface that in turn causes decrease of the net driving forces along with increase of the hydraulic permeability of membrane matrix itself;
3. Coherence between calculated and experimental profiles is observed. Estimated standard deviation of experimentally-based CP module is to be $\sigma(\alpha) = 0.02554$. Average difference between model and experimental values does not exceed 12%.
4. Membranes with moderate salt rejection rather than membrane with high salt rejections can be recommended for RO systems designed at elevated temperature (in particular for RO/MSF hybrid schemes where cooling water from heat rejection section is used as a feed for RO).

The proposed model can be used for analysis of the impact of degree of membrane rejection and temperature on polarization modulus. It can be applied for analysis and interpretation of experimental characteristics, pilot data and laboratory-scale results. It can be used for development of optimum operating conditions namely selection of preferable operating temperature against feed water quality and membrane characteristics. This

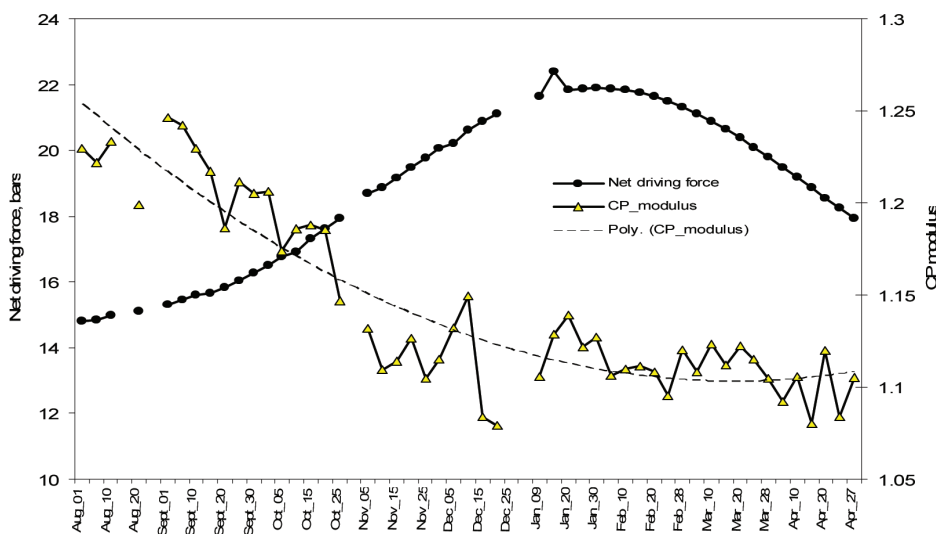


Fig. 4. Net driving force and CP modulus. (The shown profiles are based on experimental data on normalized permeability).

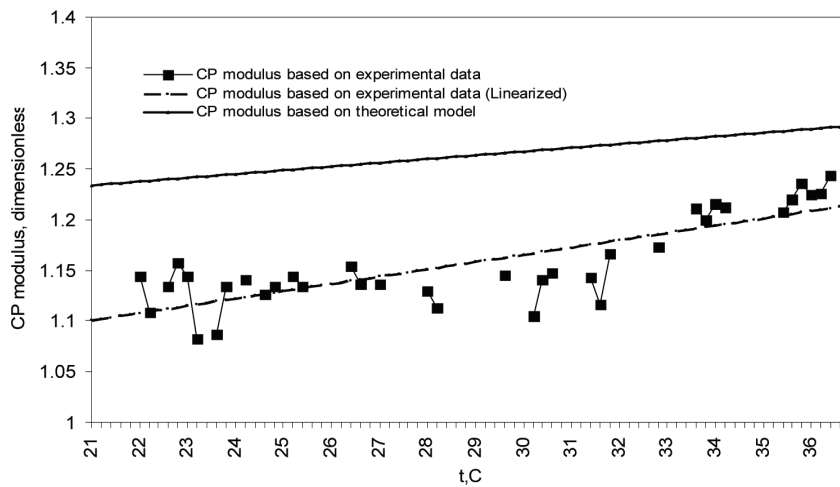


Fig. 5. Impact of temperature on polarization modulus $\alpha(t)$. Theoretical profile is based on Eqs. (6), (10), (11), (20)–(22) the experimental — on Eqs. (23)–(25).

model can be recommended for design development, it can be used for optimization of regime parameters against temperature. Along with the model can be built into an algorithm for further multidimensional optimization of the process as well.

Acknowledgements

Author is grateful to the National Energy and Water Research Center (ADWEA) for supporting this study.

Symbols and abbreviations

A_M	— Hydraulic permeability of membrane, $\text{m}^3/[\text{m}^2\text{-s-bar}]$
C	— Concentration, mol/m^3
D	— Solute diffusivity, m^2/s
f	— Upper boundary of diffusion layer, $f(t) \approx \text{Sc}(t)^{-1/3}$
H	— Half height of channel, m
P	— Operating pressure, bar
R_{OBSERVED}	— Observed degree of rejection, $R_{\text{OBSERVED}} = 1 - C_2/C_1$
R_{TRUE}	— True degree of rejection, $R_{\text{TRUE}} = 1 - C_2/C_{1M}$
Re	— The Reynolds number
Sc	— The Schmidt number
t	— Temperature, $^{\circ}\text{C}$
$V_{\text{MAX}}(V_M, V_2)$	— Transverse velocity or observed permeability, (at membrane surface and in permeated), m/s
$X(\eta)$	— Auxiliary term in Eq. (19)
z	— Vertical coordinate, m
$Z(f)$	— Auxiliary term in Eq. (19)

Greek

α	— Modulus of concentration polarization at membrane, $\alpha = C1M/C1$
δ_C	— Thickness of diffusion layer, m
δ_W	— Thickness of viscous layer, m
η	— The dimensionless variable, $\eta = (H - z)/H$
μ	— Dynamic viscosity, Pa s
π_M	— Osmotic pressure, bar
σ	— True standard deviation

Subscripts

1M	— Membrane surface
1	— High pressure (feed) channel
2	— Low pressure (permeate) channel

References

- [1] A.S. Berman, Laminar flow in channels with porous walls, *J. Appl. Physics*, 24(9) (1953) 1232–1235.
- [2] P.L. Brian, Concentration polarization in reverse osmosis desalination with variable flux and incomplete salt rejection, *I&EC Fundam.*, 4(4) (1965) 439–445.
- [3] T.K. Sherwood, R.L. Brian, R. Fisher and L. Dresner, Salt concentration at phase boundaries in desalination by RO, *I&EC Fundam.*, 4(2) (1965) 113–118.
- [4] C. Kleinstreuer and M. Paller, Laminar dilute suspension flows in plate and frame ultrafiltration units, *AEChE J.*, 29(4) (1983) 529–533.
- [5] S. Karode, Laminar flow in channel with porous walls, revisited, *J. Membr. Sci.*, 191 (2001) 237–241.
- [6] S. Karode and A. Kumar, Flow visualization through spacer filled channels by computational fluid dynamics. I. Pressure drop and shear rate calculations for flat sheet geometry, *J. Membr. Sci.*, 193 (2001) 69–84.
- [7] S. Kim and E.M.V. Hoek, Modeling concentration polarization in reverse osmosis process, *Desalination*, 186 (2005) 111–128.
- [8] D. Wiley and D. Fletcher, Techniques for computational fluid dynamics modeling of flow in membrane channel, *J. Membr. Sci.*, 211 (2003) 127–137.

- [9] V. Gupta, S.T. Hwang, W. Krantz and A. Greenberg, Characterization of nanofiltration and reverse osmosis membrane performance for aqueous and salt solutions using irreversible thermodynamics, *Desalination*, 208 (2007) 1–18.
- [10] S. Ma, L. Song, S.L. Ong and W. Ng, A 2-D streamline upwind Petrov/Galerkin finite element model for concentration polarization in spiral wound reverse osmosis modules, *J. Membr. Sci.*, 244 (2004) 129–139.
- [11] S. Delgado, R. Villarroel and E. Gonzalez, Effect of the shear intensity on fouling in submerged membrane bioreactor for wastewater treatment, *J. Membr. Sci.*, 311 (2008) 173–181.
- [12] S. Agashichev and D. Falalejev, Modeling driving force in process of ultrafiltration of non-Newtonian fluids, *J. Membr. Sci.*, 171 (2000) 173–182.
- [13] E.M.V. Hoek, A.S. Kim and M. Elimelech, Influence of cross-flow membrane filter geometry and shear rate on colloidal fouling in reverse osmosis and nano-filtration separation, *Environ. Eng. Sci.*, 19(6) (2002) 357–372.
- [14] E.M.V. Hoek and M. Elimelech, Cake enhanced concentration polarization: A new fouling mechanism for salt rejecting membranes, *Environ. Sci. Technol.*, 17 (2003) 5581–5588.
- [15] S. Agashichev, Enhancement of concentration polarization due to gel accumulated at membrane surface, *J. Membr. Sci.*, 285 (2006) 96–101.
- [16] Ch. Bellona, J. Drewes, P. Xn and G. Amy, Factors affecting the rejection of organic solutes during NF/RO treatment – a literature review, *Wat. Res.*, 38 (2004) 2795–2809.
- [17] H. Schlichting, *Grenzschicht-Theorie*, 5th ed., Verlag G. Braun, Karlsruhe, 1974.